DOI: 10.1002/ejic.200900124

Analysis of the Interaction between Adenine Nucleobase and Metal-Malonato Complexes

Sonia Pérez-Yáñez,[a] Oscar Castillo,*[a] Javier Cepeda,[a] Juan P. García-Terán,[a] Antonio Luque,*[a] and Pascual Román[a]

Keywords: Bioinorganic chemistry / Nucleobases / Supramolecular chemistry / Magnetic properties

The synthesis, crystal structure and variable-temperature magnetic measurements of compounds $[M_2(\mu\text{-Hade})_2(\mu\text{-mal})_2(H_2O)_2]\cdot 2H_2O$ [M = Ni (**1**), Co (**2**)], $[Co_2(\mu\text{-Hade})_2(\mu\text{-mal})_2(H_2O)_2]$ (**3**), $\{(H_2ade)_2[Cu(\mu\text{-mal})_2]\cdot 2H_2O\}_n$ (**4**) and $(H_2ade)_2[Cu(mmal)_2(H_2O)]$ (**5**; H_2ade = adeninium, Hade = adenine, mal = malonato, mmal = methylmalonato) are reported. Compounds **1**–**3** contain neutral paddle-wheel $[M_2(\mu\text{-Hade})_2(\mu\text{-mal})_2(H_2O)_2]$ [M = Ni (**1**), Co (**2** and **3**)] units where the 7*H*-tautomeric form of the nucleobase and the malonate dianion act as μ-κ*N3*:κ*N9* and μ-κ^2*O1*,*O2*:κ*O1* bridging ligands, respectively. The supramolecular crystal structures of **1**–**3** are essentially maintained by hydrogen-bonding interactions involving the nucleobases, the carboxylate groups and crystallisation water molecules (in compounds **1** and **2**). Compounds **4** and **5** show a hybrid inorganic-organic lamellar structure containing layers of anionic metal-malonato complexes and supramolecular aggregates of the 1*H*,9*H*-adeninium cation. Their overall three-dimensional architectures are controlled, in addition to electrostatic forces, by supramolecular recognition processes between the inorganic and organic frameworks. Compound **4** contains one-dimensional anionic copper-malonato chains in which the copper atoms are doubly bridged by μ-κ^2*O1*,*O2*:κ*O2′* malonato ligands and the cationic nucleobases form dimeric entities sustained by Hoogsteen-Hoogsteen hydrogen-bonding interactions. Compound **5** is built up of anionic $[Cu(mmal)_2(H_2O)]^{2-}$ monomeric entities and planar, hydrogen-bonded, one-dimensional, ribbon-like aggregates of protonated adenine. Variable-temperature magnetic susceptibility measurements of compounds **1**–**4** show the preponderance of ferromagnetic interactions between the paramagnetic centres. DFT calculations have been performed to evaluate the magnetic behaviour of these compounds and to analyze the interaction between two adeninium cations in compound **4**.

Introduction

Over the past decades substantial research effort has been invested in the rational design and elaboration of biomimetic systems[1] based on the interaction of nucleic acids and their building units with a wide range of both organic and inorganic frameworks.[2] The interest in these systems not only stems from the desire to better understand the complex interactions often present in a great diversity of molecular biorecognition processes[3] but also to afford a powerful tool for the improvement of pharmaceutical agents[4] and the development of artificial receptors used as specific nucleotide sensors or even for the determination of low concentrations of biological and therapeutic agents.[5]

Our research group has recently demonstrated the high efficiency of several metal-oxalato systems to act as receptors of adenine and cytosine (neutral, cationic and supramolecular aggregates) by means of the covalent anchoring of nucleobases to the metal centres and/or by the establishment of complex hydrogen-bonding recognition patterns between the organic and inorganic frameworks.[6] Now we have extended this work to the malonate anion, a ligand with a greater flexibility that gives a more extended structural diversity. This ligand has a remarkable versatility in adopting several different modes of bonding, including monodentate, chelating and bridging, with more than one of these modes sometimes occurring in the same compound.[7]

We report herein the synthesis, crystal structure and variable-temperature magnetic measurements of five compounds containing the nucleobase adenine and a malonato ligand, namely $[M_2(\mu\text{-Hade})_2(\mu\text{-mal})_2(H_2O)_2]\cdot 2H_2O$ [M = Ni (**1**), Co (**2**)], $[Co_2(\mu\text{-Hade})_2(\mu\text{-mal})_2(H_2O)_2]$ (**3**), $\{(H_2ade)_2[Cu(\mu\text{-mal})_2]\cdot 2H_2O\}_n$ (**4**) and $(H_2ade)_2[Cu(mmal)_2(H_2O)]$ (**5**) (H_2ade = adeninium, Hade = adenine, mal = malonato, mmal = methylmalonato), and demonstrate that the metal-malonato frameworks, as well as the metal-oxalato systems, act as adenine receptors.

Compounds **1**–**3** contain pseudo-structural "paddle-wheel" dinuclear units in which the nucleobase is in the 7*H*-adenine form. Since the first example of this kind of arrangement, $[Cu_2(\mu\text{-adenine})_4(H_2O)_2]\cdot 5H_2O$, was reported by Sletten,[8] a great deal of attention has been paid to the

[a] Departamento de Química Inorgánica, Facultad de Ciencia y Tecnología, Universidad del País Vasco,
Apartado 644, 48080 Bilbao, Spain
Fax: +34-94-601-3500
E-mail: oscar.castillo@ehu.es
antonio.luque@ehu.es

design of compounds containing $[M_2(\mu\text{-adenine})_{4-x}(L)_x]$ frameworks with different ligands due both to their potential ability to act as building blocks in the construction of supramolecular architectures[9] and because they are possible candidates for anticancer treatment, as has been discussed both theoretically and experimentally.[10] Compounds **4** and **5** are lamellar hybrid structures formed by alternating inorganic and organic layers. Hybrid inorganic-organic compounds have attracted an increasing interest over the last few years due to the possibility of combining the different characteristic of the components to achieve unusual structures, properties or applications (catalysis, gas separation and storage) which are not commonly observed in purely inorganic or organic phases.[11]

Results and Discussion

$[M_2(\mu\text{-Hade})_2(\mu\text{-mal})_2(H_2O)_2]\cdot 2H_2O$ [M = Ni (1), Co (2)] and $[Co_2(\mu\text{-Hade})_2(\mu\text{-mal})_2(H_2O)_2]$ (3)

X-ray diffraction analysis of compounds **1**–**3** showed that their crystal structures consist of centrosymmetric $[M_2(\mu\text{-Hade})_2(\mu\text{-mal})_2(H_2O)_2]$ [M = Ni (**1**), Co (**2**), Co (**3**)] units and crystallisation water molecules (in compounds **1** and **2**). A perspective view of the structural units of compound **1**, with the atomic numbering scheme, is given in Figure 1.

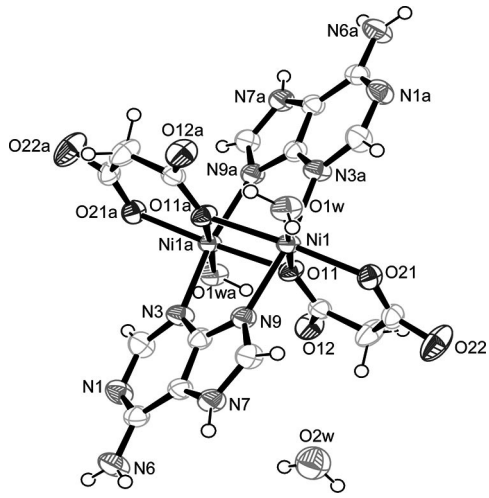

Figure 1. Structural units of compound **1** with the atomic numbering scheme.

The metal centres within the dinuclear entities are bridged by two malonate anions and two neutral adenine molecules to give a paddle-wheel motif. Each metal is coordinated to three oxygen atoms from the malonato ligands and two nitrogen atoms of adenine nucleobases. The octahedral distorted polyhedron is completed with a water molecule to give an N_2O_3Ow donor set. Selected bond lengths for the coordination polyhedron are listed in Table 1.

Table 1. Selected bond lengths [Å] for the coordination polyhedron of compounds **1**–**3**.[a]

	1	**2**	**3**
M1–N3a	2.082(3)	2.145(4)	2.191(4)
M1–N9	2.074(3)	2.144(5)	2.108(5)
M1–O11	2.021(2)	2.061(4)	2.144(4)
M1–O11a	2.073(2)	2.115(5)	2.105(4)
M1–O21	2.003(2)	2.037(5)	2.032(4)
M1–O1w	2.047(2)	2.093(3)	2.018(3)

[a] Symmetry codes: (a) $1-x, -y, 1-z$ (for **1**, **2**); (a) $1-x, -y, -z$ (for **3**).

The malonate anion shows an unusual tridentate μ-$\kappa^2 O1,O2$:$\kappa O1$ coordination mode where O11 links both metal atoms and O21 is only bonded to one of these metal centres, thus forming a six-membered chelate ring.[12] The two carboxylato groups of the malonato ligands in compound **3** are tilted 40.8°. This distortion can be attributed to more restrictive requirements of the molecular interactions due to the absence of crystallisation water molecules to mediate them. The adenine bridging ligand is attached to one metal centre by means of the pyrimidinic N3 atom and to the other one through the N9 atom of the imidazolic ring to give a μ-$\kappa N3$:$\kappa N9$ coordination mode. Unlike in compounds **1** and **2**, the two bridging adenine ligands in compound **3** are not coplanar (0.371 Å between their mean planes). The M···M distances [2.997(1), 3.047(1) and 3.051(1) Å for **1**–**3**, respectively] are similar to those reported for analogous "paddle-wheel" $[Cu_2(\mu\text{-adenine})_4(X)_2]$ dinuclear units containing this bridging ligand.[8,13] Although there are no reported examples of the adenine μ-$\kappa N3$:$\kappa N9$ coordination mode with nickel or cobalt, Klanicová et al. have recently reported the crystal structure of a compound containing a paddle-wheel dimeric fragment in which cobalt(II) atoms are joined by two 6-(4-fluorobenzylamino)purinato bridging ligands with a Co···Co distance of 2.667 Å.[14] The metal atoms in the above cited "paddle-wheel" copper complexes are pentacoordinate and the M–X axial bonds (X = Cl, H_2O) are almost collinear with the Cu···Cu axis. The metal centres in compounds **1**–**3** are hexacoordinate and the angles between the M–O1w bond and the metal···metal axis are 44.9°, 44.3° and 34.5°, respectively. This bending allows the formation of an intramolecular O1w–H11w···O12a hydrogen bond in compounds **1** and **2**, or may be a consequence thereof.

Coordination of the adenine through N9 of the pyrimidinic ring results in stabilisation of the 7*H*-adenine tautomer, which is its most usual form in complexes where the nucleobase behaves as either an N9-monodentate or N3,N9-bridging ligand. The 7*H*-adenine tautomer is additionally stabilized in compounds **1** and **2** by the formation of an $R^2_2(9)$ ring formed by doubly hydrogen-bonding interactions between the Hoogsteen face and the carboxylate group of an adjacent dimeric unit. Similar nine-membered rings involving the Hoogsteen face of the adenine nucleobase are common in both artificial and biological systems, but most of them imply O/N–H···N7 interactions with the N7 site as H-bond acceptor.[15] Hoogsteen AT base-pairings found in

different structures of DNA and RNA[16] and the Asn/Glu-adenine interaction in protein-nucleic acid complexes[17] are sustained by this kind of hydrogen-bonded ring.

The Watson–Crick face of the nucleobase in compounds **1** and **2** is hydrogen-bonded to an oxygen atom of another dinuclear entity as donor, and to a crystallisation water molecule as acceptor. This water molecule establishes a second hydrogen bond with a coordinated water molecule of an adjacent dimer, thus giving rise to layers of complex units in the *bc* plane (Figure 2a). The dimeric units within these layers adopt two different orientations, with an angle of around 40°, thus forming a rhombic net. The dimeric layers are joined together through a hydrogen-bonding interaction involving O22 of a malonato ligand and a crystallisation water molecule of an adjacent layer. No significant π–π interactions have been observed.

The supramolecular crystal structure of compound **3** is different to that described for compounds **1**–**2** due to the absence of crystallisation water molecules. In this case, the Hoogsteen face is hydrogen-bonded to the O12 oxygen atom of the carboxylate group of an adjacent dimeric unit, which results in the formation of an $R^1_2(7)$ hydrogen-bonding ring. These interactions lead to unidimensional chains that run along the [100] direction. The interaction of the Watson–Crick face, which acts only as a hydrogen-bond donor (N6–H61···O21), together with those involving the coordinated water molecules, gives rise to layers joined together through hydrogen-bonding interactions (Figure 2b).

$\{(H_2ade)_2[Cu(\mu\text{-}mal)_2]\cdot 2H_2O\}_n$ (4)

The crystal structure of complex **4** is made up of copper-malonato chains, adeninium cations and crystallisation

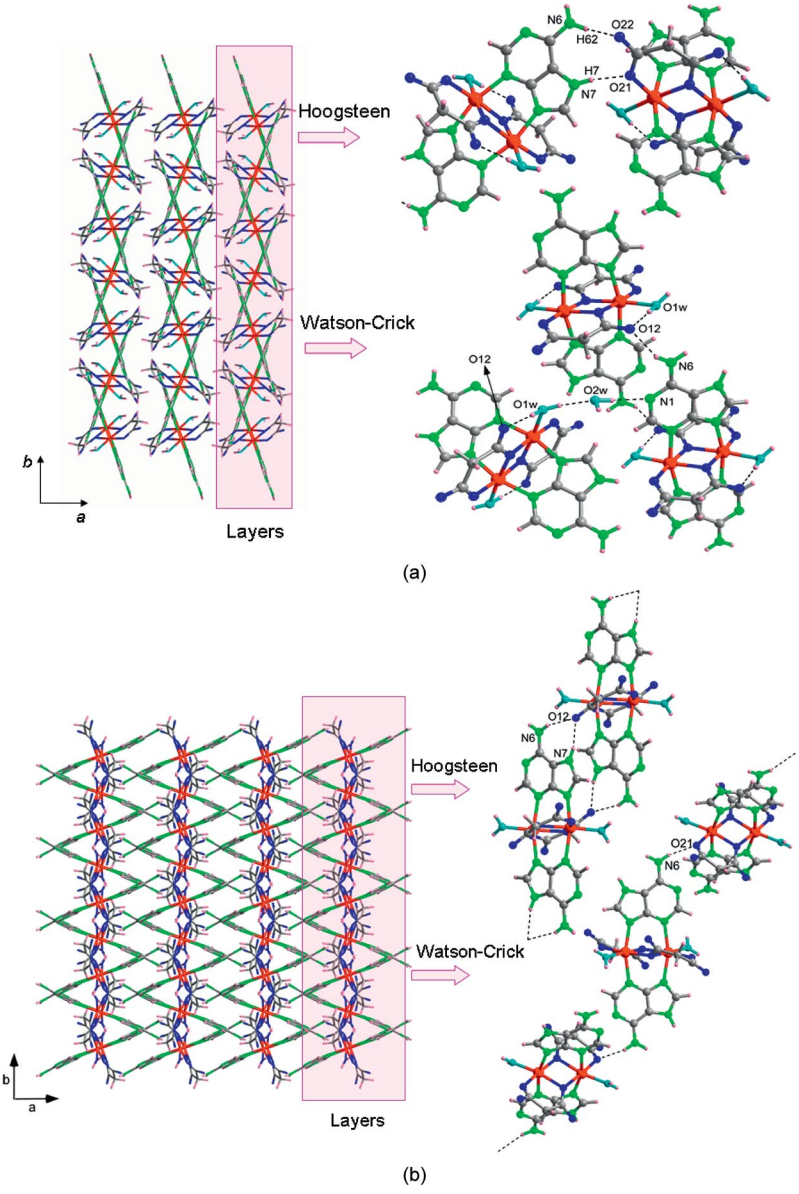

Figure 2. Supramolecular structures of compounds **1** and **2** (a) and compound **3** (b).

water molecules held together by electrostatic and hydrogen-bonding interactions (Figure 3).

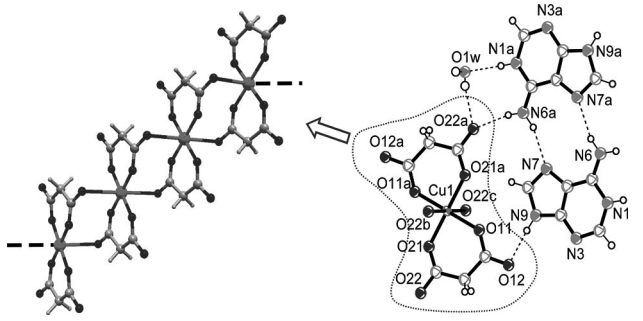

Figure 3. Structural units of compound **4** showing the 1D anionic chain and the hydrogen-bonding interactions (dashed lines).

The copper-malonato chains are made up of $[Cu(mal)_2]^{2-}$ anionic units that stack up along the [100] direction. The copper atoms are placed on an inversion centre and are surrounded by six oxygen atoms from four different malonato groups to form an elongated octahedral environment. Four coplanar oxygen atoms from two bidentate malonato ligands form the equatorial plane around the copper atom, giving rise to a six-membered chelate ring, while the apical positions are filled by two carboxylate oxygen atoms, which are not involved in the chelation, from two neighbouring $[Cu(mal)_2]^{2-}$ units. The apical Cu–O bond length is significantly longer [2.705(2) Å] than the equatorial ones [1.923(2) and 1.928(2) Å]. Selected bond lengths and angles for the coordination polyhedron are listed in Table 2. Each malonate anion acts as a bidentate μ-κ^2*O1*,*O2*:κ*O2′* bridging ligand and connects an equatorial site of one copper atom with the apical site of an adjacent one with a copper···copper separation through the carboxylate bridge of 5.081 Å.

Table 2. Selected bond lengths [Å] and angles [°] for the coordination polyhedron of compound **4**.[a]

Cu1–O11	1.923(2)	Cu1–O22b	2.705(2)
Cu1–O21	1.928(2)		
O11–Cu1–O11a	180.0(–)	O21–Cu1–O21a	180.0(–)
O11–Cu1–O21	93.30(8)	O21–Cu1–O22b	89.78(7)
O11–Cu1–O21a	86.70(8)	O21–Cu1–O22c	90.22(7)
O11–Cu1–O22b	86.99(7)	O22b–Cu1–O22c	180.0(–)
O11–Cu1–O22c	93.01(7)		

[a] Symmetry codes: (a) $1 - x, -y, 1 - z$; (b) $x - 1, y, z$; (c) $2 - x, -y, 1 - z$.

The polymeric chains are hydrogen-bonded to the crystallisation water molecules, which leads to the formation of anionic inorganic layers that propagate in the *ab* plane. The outside of these layers is made up of the oxygen atoms of the malonato ligands and the crystallisation water molecules, which make them optimum acceptors for molecules with a high number of potential hydrogen-bonding donor positions, as is the case of the 1*H*,9*H*-adeninium cations. These cations are inserted between the anionic sheets, and they interact through their Watson–Crick face with one of these sheets and through the N9 atom of the imidazolic ring with the other one (Figure 4). The organic-inorganic interaction is reinforced by weak C–H···O hydrogen bonds. The Watson–Crick face establishes an $R^2_3(8)$ hydrogen-bonded ring similar to that found in the crystalline structure of 1*H*,9*H*-adeninium chloroanilate dihydrate[18] but exchanging the water molecule and C=O group positions. It also resembles that found in the end cap of the binding pocket of the vaccinia VP39 virus protein used to discriminate between alkylated and nonalkylated nucleobases.[19]

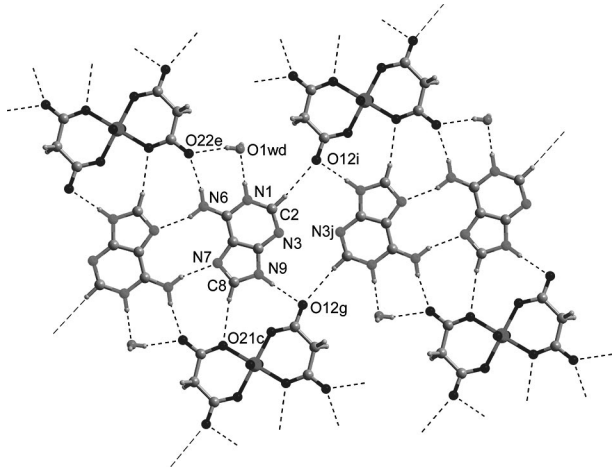

Figure 4. Insertion of the protonated nucleobases between the inorganic layers.

As a result of the interaction with the inorganic sheets, the Hoogsteen face of adeninium is free to establish a double N6–H6···N7 interaction with an adjacent cation to form dimeric aggregates. These aggregates spread out along the [210] direction in such a way that the lone pairs of the nitrogen N3 atoms from adjacent aggregates lie face to face, at a distance of 3.24 Å, without any other interaction between the aggregates that could explain this unusual disposition. A similar arrangement of the pyrimidinic N3 atom in adenine in relation to the aromatic nitrogen atoms has been described when bis(benzimidazole) groups of organic molecules anchor to polynucleotides in a non-planar disposition of nucleobase and aromatic ring,[20] although in this case it is due to the presence of additional non-covalent interactions. The observed disposition of the adeniniun cations facing their N3 atoms is therefore probably due to structural requirements of the crystal packing of compound **4**, which is sustained by the hydrogen-bonding network involving the adeninium cations and the anionic $[Cu(\mu\text{-}mal)_2]_n^{2n-}$ complex entities.

B3LYP geometric optimisations were performed to gain a deeper insight into the adeninium-adeninium interactions. The optimisation of a model based on the crystallographic structural data with only two adeninium cations facing their N3 atoms, without any symmetry restraints, moves the cations away. However, the initial disposition is maintained if we simulate the interactions that are present in the crystal structure between two opposing cations by means of the formaldehyde molecule, although the N3···N3 distance increases (3.8 Å). This fact seems to point to the crystal

framework being responsible for the approach between cations instead of an interaction between the lone pairs.

In conclusion, the supramolecular structure of **4** is built up by three types of molecular recognition patterns: a) between metal-malonato chains and water molecules, b) between anionic chains and adeninium cations and c) between adeninium cations (Figure 5). Anionic chains and water molecules are bound by hydrogen-bonding interactions, which gives rise to an anionic layer. Secondly, organic cations, which interact non-covalently with these chains, occupy the interlayer space. Finally, the molecular recognition among the adeninium cations results in double-faced hydrogen-bonded aggregates.

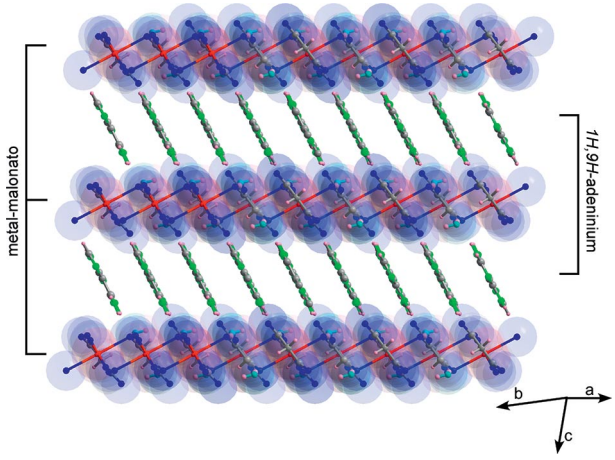

Figure 5. Packing of compound **4** showing the alternating inorganic and organic layers along the [210] direction.

$(H_2ade)_2[Cu(mmal)_2(H_2O)]$ (5)

The crystallographic analysis of complex **5** showed that its structure consists of monomeric $[Cu(mmal)_2(H_2O)]^{2-}$ entities and adeninium cations held together by electrostatic and hydrogen-bonding interactions (Figure 6a). The Cu^{II} atom within the complex unit exhibits a square-pyramidal environment (4+1) with four oxygen atoms belonging to two chelating methylmalonate anions in the basal plane and one water molecule filling the apical position (Table 3). The steric hindrance of the methyl group of the malonato ligand, which is oriented outwards from the anionic complex, causes the non-planarity of the dicarboxylate.[21]

Table 3. Selected bond lengths [Å] and angles [°] for compound **5**.[a]

Cu1–O11	1.960(1)	Cu1–O1w	2.265(2)
Cu1–O21	1.927(1)		
O11–Cu1–O11a	91.68(7)	O21–Cu1–O21a	91.20(8)
O11–Cu1–O21	86.57(5)	O11–Cu1–O21a	164.87(6)
O11–Cu1–O1w	99.67(5)	O21–Cu1–O1w	95.44(6)

[a] Symmetry code: (a) x, $-y + 1/2$, z.

The monomers are connected by means of [O1w–H11w···O12] hydrogen bonds between the coordinated water molecule and the oxygen atoms of one of the methylmalonato ligand that are not implicated in the metal chelation, leading to *zigzag* ribbons running along the [100] direction (Figure 6b).

The 1*H*,9*H*-adeninium cations generate cationic ribbons running along the [001] direction by means of $R^2_2(8)$ hydrogen-bonding interactions between the Hoogsteen face of a cation and the C2 and N3 atoms of a neighbouring adeninium cation (Figure 6c). These cationic ribbons are inserted between the anionic layers with a crossing angle between the inorganic and organic ribbons of 90°.

The outer face of the cationic ribbons alternately exposes the sugar and Watson–Crick sides of the protonated nucleobases. This arrangement allows a strong interaction with the complex anionic ribbons that involves the Watson–Crick side and the O–Cu–O fragment, which establish an $R^2_2(8)$ hydrogen-bonded ring, and on the other side the N9 donor-site and the non-coordinated oxygen atom of a methylmalonato ligand belonging to a second anionic ribbon. A similar interaction involving the Watson–Crick side and O–Cu–O group has been described previously to be the most stable among the possibilities where the oxalato anion acts as metal-bonding ligand.[22] This overall hydrogen-bonding

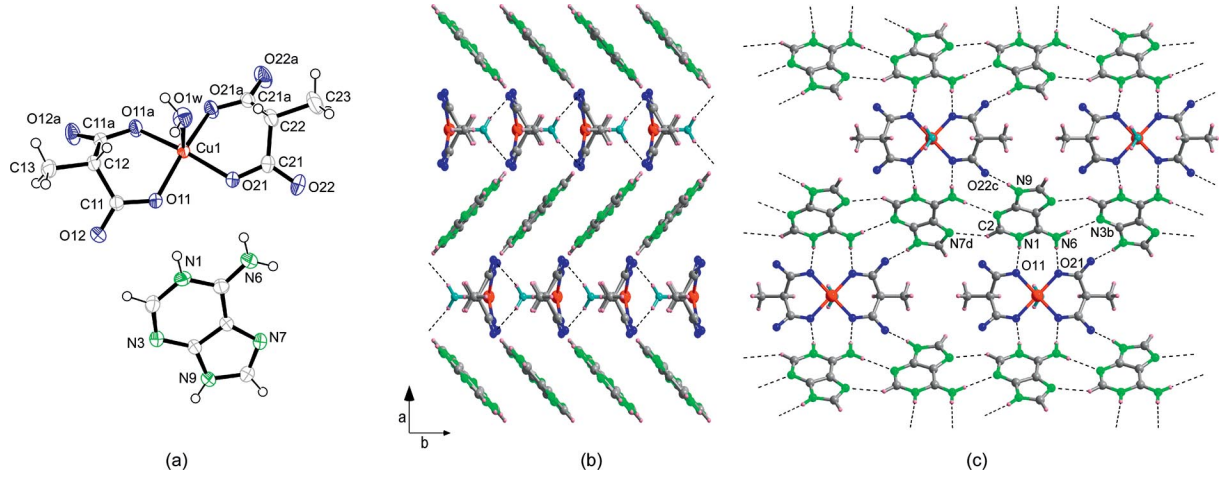

Figure 6. (a) Structural units of compound **5** with the atomic numbering scheme; (b) view along the [001] direction showing the lamellar structure; (c) hydrogen-bonding interactions between the inorganic and organic frameworks.

scheme leads to an inorganic-organic lamellar arrangement, although no significant interaction is observed between ribbons belonging to the same sheet (Figure 6c).

Magnetic Properties

The magnetic behaviour of **1** in the form of a $\chi_M T$ vs. T plot [χ_M being the magnetic susceptibility per nickel(II) ion] is shown in Figure 7. Upon cooling, $\chi_M T$ increases progressively to reach a maximum at 10 K, and then decreases quickly. This behaviour is characteristic of a nickel dimer with a weak ferromagnetic interaction. The decrease observed at low temperatures could be due to either zero field splitting and/or the presence of antiferromagnetic interactions along the dimeric entities. However, taking into account the long intermolecular Ni···Ni distance (greater than 7.1 Å), this decrease is probably due to zero field splitting. The room-temperature $\chi_M T$ value is equal to 1.33 $cm^3 mol^{-1}$, a value which is close to that expected for a magnetically isolated spin doublet (1.00 $cm^3 mol^{-1}$, with $g = 2$). The magnetic data were successfully fitted by the numerical expression proposed by Ginsberg for dimers of $S = 1$ ions,[23] which includes the zero field splitting effect in the paramagnetic centres. The best fit of the magnetic data leads to $J = +14.4$ cm^{-1}, $g = 2.18$ and $|D| = 5.5$ cm^{-1}.

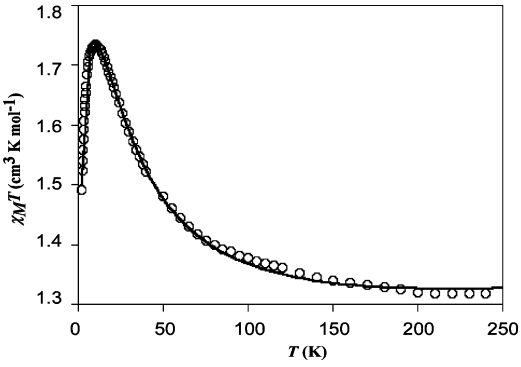

Figure 7. Thermal dependence of $\chi_M T$ (o) for compound **1**. (–) best theoretical fit (see text).

It is well known that non-linear NCN bridges cause antiferromagnetic coupling[24] while μ-oxo bridges are able to transmit both ferromagnetic and antiferromagnetic interactions depending on the M–O–M angle and the orientation of the metal-centred magnetic orbitals.[25] However, the coexistence of these two types of bridges requires a more exhaustive analysis than when there is only one type. In fact, when the bridging ligands are different, the two bridges may either add or counterbalance their effects. This problem has been treated by Nishida et al.[26] and McKee et al.,[27] and these phenomena are known as orbital complementarity and countercomplementarity, respectively. In the present case, the splitting of the molecular magnetic orbitals is reversed for each type of bridging ligand, thus leading an almost negligible energy difference between them (see qualitative MO diagram in Scheme 1). This small energy difference is responsible for the observed ferromagnetic behaviour of compound **1**.

This conclusion was reinforced by DFTUB3LYP calculations of the J parameter performed on an isolated dimer model based on the crystal structure, which gives a value of +20.0 cm^{-1}. This value fits fairly well the experimental one (+14.4 cm^{-1}) with an acceptable deviation for this kind of calculation. The calculated spin-density distribution for the singlet state of compound **1** is shown in Figure 8.

The magnetic behaviours of **2** and **3** in the form of $\chi_M T$ vs. T plots [χ_M is the magnetic susceptibility per cobalt(II) ion] are shown in Figure 9. At room temperature, $\chi_M T$ is equal to 2.7 (**2**) and 2.9 $cm^3 mol^{-1} K$ (**3**), values which are slightly greater than that expected for two magnetically isolated spin triplets ($\chi_M T = 2.43$ $cm^3 mol^{-1} K$). The experimental magnetic data for compounds **2** and **3** were fitted with the Lines theory[28] for polynuclear cobalt(II) compounds, which takes into account the orbital reduction factor (κ) and the spin-orbit coupling parameter (λ) together with the magnetic coupling (J). Unfortunately, the fitting process did not reproduce the experimental curves satisfactorily and, as a consequence, we are unable to provide reliable magnetic coupling constants for these two complexes. Nevertheless, the characteristics of the curve, which clearly shows an increase of $\chi_M T$ with temperature decrease for compound **2**, indicate a net ferromagnetic interaction within the dimeric entity. The absence of an increase in the $\chi_M T$ curve in compound **3** could be compatible with antiferromagnetic or even weak ferromagnetic interactions hidden by the spin-orbit coupling effect. In order to provide further insights, DFTUB3LYP calculations of the J parameter performed on dimeric models based on the crystallographic data lead to values of $J = +6.0$ cm^{-1} (**2**) and $J = +1.09$ cm^{-1} (**3**), in good agreement with those reported previously. These values can be interpreted as a consequence of the previously described counterbalance effect between the adenine and malonato bridging ligands.

The magnetic behaviour of **4** in the form of a $\chi_M T$ vs. T plot [χ_M is the magnetic susceptibility per copper(II) ion] is shown in Figure 10. The room-temperature $\chi_M T$ value (0.42 $cm^3 mol^{-1}$) is close to that expected for a magnetically isolated spin doublet (0.375 $cm^3 mol^{-1}$). Upon cooling, $\chi_M T$ remains practically constant down to 50 K, and then increases smoothly at lower temperatures, reaching a value of 0.50 $cm^3 mol^{-1}$ at 4 K. This curve reveals the occurrence of an overall weak ferromagnetic interaction. As the structure of **4** is made up of uniform chains of $[Cu(mal)_2]_n^{2n-}$ units which are well separated from each other by large 1*H*,9*H*-adeninium cations, its magnetic data can be analysed through the numerical expression for a ferromagnetically coupled regular chain of local spin doublets.[29] The best fit of the magnetic data leads to $J = +0.6$ cm^{-1} and $g = 2.11$.

In order to gain a deeper insight into the magnetic properties of compound **4**, DFTUB3LYP calculations were performed on an isolated dimer model based on its crystal structure where the axial oxygen atoms are replaced by water molecules. The obtained value ($J = +1.1$ cm^{-1}) is in good agreement with the experimental one. In good agreement with the elongated six-coordinate environment observed for the Cu1 atom in compound **4**, the unpaired elec-

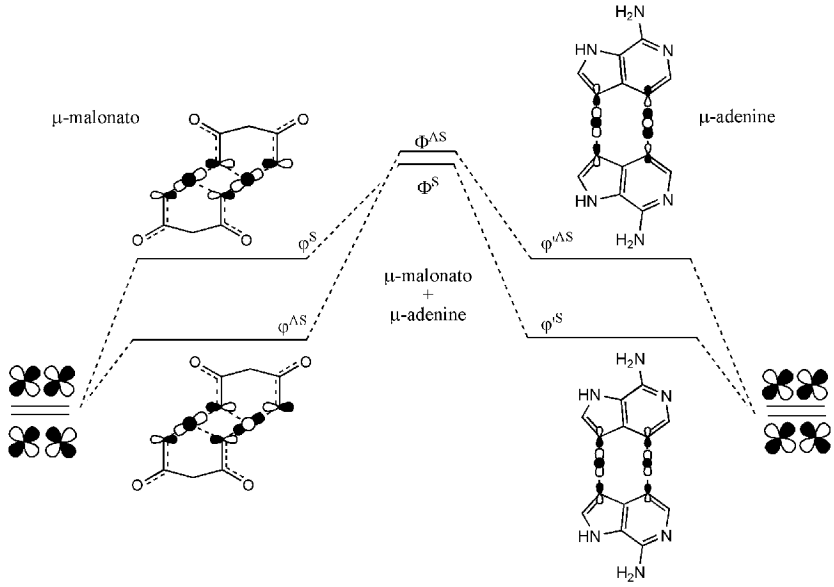

Scheme 1. Energy splitting of the $d_{x^2-y^2}$-based magnetic orbitals.

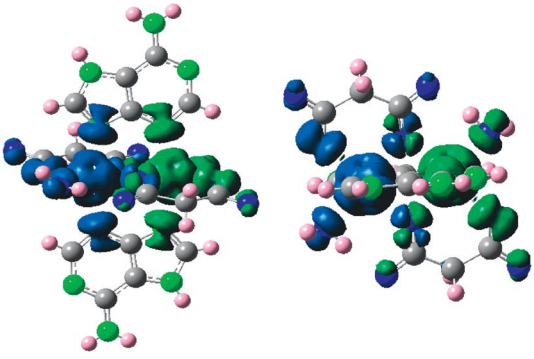

Figure 8. Spin-density distribution for the singlet state of compound **1**.

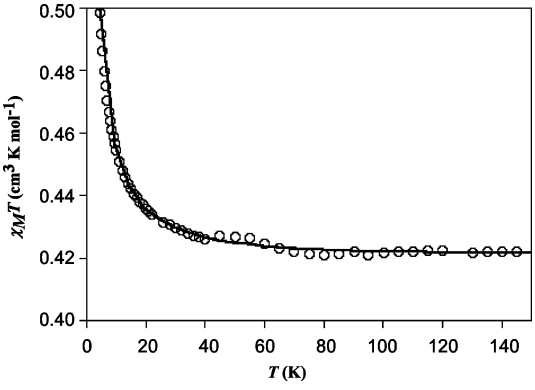

Figure 10. Thermal dependence of $\chi_M T$ (o) for compound **4**. (–) best theoretical fit (see text).

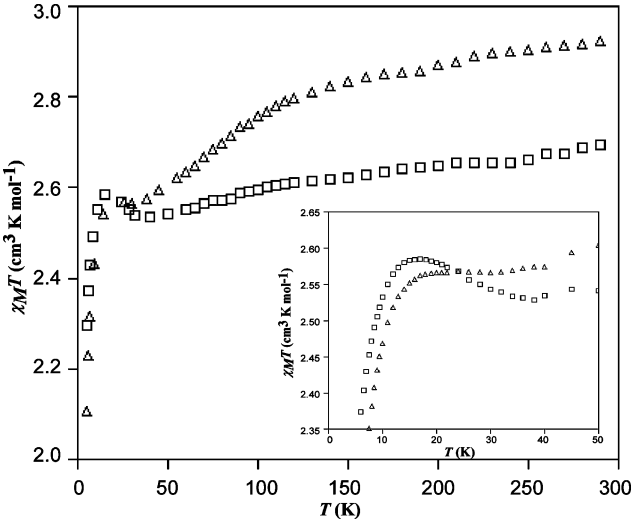

Figure 9. Thermal dependence of $\chi_M T$ for compounds **2** (□) and **3** (Δ).

tron is mainly located in the equatorial plane, which is of the $d_{x^2-y^2}$ type (magnetic orbital) [the *x* and *y* axes are roughly defined by the Cu1–O21 and Cu1–O11 bonds]. A weak spin is thus expected in the apical positions. As the intrachain exchange pathway in **4** involves the equatorial–apical connection through a carboxylato bridge [Cu1–O21–C13–O22···Cu1d], the overlap (*S*) between the magnetic orbitals of Cu1 and Cu1d is predicted to be very small or zero (accidental orthogonality). Given that the magnitude of the antiferromagnetic interaction in a copper(II) dimer is proportional to S^2,[30] the ferromagnetic contribution is expected to be dominant, which means that the resulting magnetic coupling in **4** is most likely ferromagnetic, as observed. In addition, previous experimental and theoretical studies of carboxylato-bridged copper(II) complexes have shown that the value of the exchange coupling between copper(II) ions through the bridging carboxylato is strongly dependent on the bridging mode of the carboxylate (*syn–syn*, *anti–anti* and *anti–syn*) and the type of Cu–O–C–O–Cu

pathway involved (equatorial–equatorial or equatorial–apical). Finally, the value of the ferromagnetic coupling observed in compound **4** ($J = +0.6\ cm^{-1}$) is similar to those reported for the same orientations of the bridge and magnetic orbitals.[31]

Conclusions

This work has proved that metal-malonato fragments are good receptors for neutral (**1**–**3**) and protonated adenine (**4** and **5**) molecules. The obtained compounds reveal that the neutral nucleobase is able to coordinate the metal centre and gives rise to dimeric complexes in which both the malonato and adenine act as bridging ligands. The presence of adenine bridges imposes a metal···metal distance which is appropriate for the unusual bridging mode of the malonate anion.

The large number of hydrogen-bond acceptor positions of the metal-malonato fragments, together with the high capacity of the adeninium cations to act as hydrogen-bond donors, allows their self-anchoring.

The observed ferromagnetic behaviour of these compounds is attributed to an orbital countercomplementarity of the adenine and malonato bridges for nickel and cobalt dimers, and to an accidental orthogonality between the magnetic orbitals for the 1D copper complex.

Experimental Section

Reagents: All chemicals were of reagent grade and were used as commercially obtained.

Physical Measurements: Elemental analyses (C,H,N) were performed with a Perkin–Elmer Analyst 100 microanalytical analyser. Metal content was determined by absorption spectrometry. The IR spectra (KBr pellets) were recorded with a FTIR 8400S Shimadzu spectrometer in the 4000–400 cm^{-1} spectral region. Magnetic measurements were performed on polycrystalline samples of the complexes taken from the same uniform batches used for the structural determinations with a Quantum Design SQUID susceptometer covering the temperature range 5.0–300 K at a magnetic field of 1000 G. The susceptibility data were corrected for the diamagnetism, as estimated from Pascal's tables,[32] the temperature-independent paramagnetism and the magnetisation of the sample holder.

Synthesis of $[Ni_2(\mu\text{-Hade})_2(\mu\text{-mal})_2(H_2O)_2]\cdot 2H_2O$ (1): An aqueous solution (3 mL) of $Ni(NO_3)_2\cdot 6H_2O$ (0.0596 g, 0.2 mmol) was added dropwise to an aqueous solution (13 mL) containing malonic acid (0.1061 g, 1 mmol) and adenine (0.0274 g, 0.2 mmol) with continuous stirring at 80 °C. The resulting solution (pH 1.9) was neutralised with NaOH to obtain a pH of 6.0. Light green X-ray quality single-crystals were obtained by slow evaporation after three days. Yield (based on metal): 39.8 mg (0.12 mmol, 60%). $C_8H_{11}N_5NiO_6$ (331.91): calcd. C 28.95, H 3.34, N 21.10, Ni 17.68; found C 29.06, H 3.27, N 20.91, Ni 17.73. Selected IR data (KBr pellet): $\tilde{\nu}$ = 3416 s [ν(O–H)]; 3366 s [$\nu(NH_2) + 2\delta(NH_2)$]; 3148 m [$\nu(C^8–H + C^2–H)$]; 1685 s [$\nu_{as}$(O–C–O)]; 1623 s, 1600 s [ν(C=C) + $\delta(NH_2)$]; 1561 s, 1525 sh [$\nu(C^4–C^5) + \nu(N^3–C^4–C^5)$]; 1475 m, 1427 m [$\delta(C^2–H + C^8–N^9) + \nu(C^8–H)$]; 1408 m [$\delta(N^1–C^6–H^6)$]; 1366 m [$\nu(C^5–N^7–C^8)$]; 1283 m [$\nu(N^9–C^8 + N^3–C^2) + \delta$(C–H) + ν_s(O–C–O)]; 1260 m, 1180 w, 1124 w [$\delta(C^8–H) + \nu(N^7–C^8)$]; 1025 m [$\tau(NH_2)$]; 955 m, 924 m [$\nu(N^1–C^6) + \tau(NH_2)$]; 853 w, 779 w [$\delta$(O–C–O)]; 725 m, 610 m (ring deformation); 550 w [ν(M–O + M–N)].

Synthesis of $[Co_2(\mu\text{-Hade})_2(\mu\text{-mal})_2(H_2O)_2]\cdot 2H_2O$ (2) and $[Co_2(\mu\text{-Hade})_2(\mu\text{-mal})_2(H_2O)_2]$ (3): An aqueous solution (2 mL) of $Co(NO_3)_2\cdot 6H_2O$ (0.0586 g, 0.2 mmol) was added dropwise to an aqueous solution (18 mL) containing $Na_2C_3H_2O_4\cdot H_2O$ (0.0505 g, 0.3 mmol) and adenine (0.0542 g, 0.4 mmol) with continuous stirring at 80 °C (pH 6.7). A mixture of light pink (**2**) and dark pink (**3**) single-crystals suitable for X-ray determination was obtained after two months by slow evaporation. Due to their colour and morphological differences, they were manually separated and the purity of the samples obtained was analysed by X-ray powder diffraction.

Compound 2: Yield 13.3 mg (0.04 mmol, 20%). $C_8H_{11}CoN_5O_6$ (332.15): calcd. C 28.93, H 3.34, Co 17.74, N 21.09; found C 29.07, H 3.43, Co 17.81, N 20.81. Selected IR data (KBr pellet): $\tilde{\nu}$ = 3416 s [ν(O–H)]; 3366 s [$\nu(NH_2) + 2\delta(NH_2)$]; 3155 m [$\nu(C^8–H + C^2–H)$]; 1685 s [$\nu_{as}$(O–C–O)]; 1625 s, 1601 s [ν(C=C) + $\delta(NH_2)$]; 1564 s, 1521 sh [$\nu(C^4–C^5) + \nu(N^3–C^4–C^5)$]; 1471 m, 1425 m [$\delta(C^2–H + C^8–N^9) + \nu(C^8–H)$]; 1406 m [$\delta(N^1–C^6–H^6)$]; 1365 m [$\nu(C^5–N^7–C^8)$]; 1284 m [$\nu(N^9–C^8 + N^3–C^2) + \delta$(C–H) + ν_s(O–C–O)]; 1261 m, 1183 w, 1126 w [$\delta(C^8–H) + \nu(N^7–C^8)$]; 1023 m [$\tau(NH_2)$]; 955 m, 920 m [$\nu$(N1–C6) + $\tau(NH_2)$]; 854 w, 795 w [δ(O–C–O)]; 721 m, 609 m (ring deformation); 550 w [ν(M–O + M–N)].

Compound 3: Yield 31.4 mg (0.10 mmol, 50%). $C_8H_9CoN_5O_5$ (314.13): calcd. C 30.59, H 2.89, Co 18.76, N 22.30; found C 30.71, H 2.95, Co 18.47, N 21.94. Selected IR data (KBr pellet): $\tilde{\nu}$ = 3413 s [ν(O–H)]; 3368 s [$\nu(NH_2) + 2\delta(NH_2)$]; 3150 m [$\nu(C^8–H + C^2–H)$]; 1682 s [$\nu_{as}$(O–C–O)]; 1621 s, 1600 s [ν(C=C) + $\delta(NH_2)$]; 1561 s, 1523 sh [$\nu(C^4–C^5) + \nu(N^3–C^4–C^5)$]; 1475 m, 1423 m [$\delta(C^2–H + C^8–N^9) + \nu(C^8–H)$]; 1408 m [$\delta(N^1–C^6–H^6)$]; 1362 m [$\nu(C^5–N^7–C^8)$]; 1281 m [$\nu(N^9–C^8 + N^3–C^2) + \delta$(C–H) + ν_s(O–C–O)]; 1260 m, 1189 w, 1128 w [$\delta(C^8–H) + \nu(N^7–C^8)$]; 1027 m [$\tau(NH_2)$]; 957 m, 918 m [$\nu$(N1–C6) + $\tau(NH_2)$]; 850 w, 797 w [δ(O–C–O)]; 726 m, 606 m (ring deformation); 549 w [ν(M–O + M–N)].

Synthesis of $\{(H_2ade)_2[Cu(\mu\text{-mal})_2]\cdot 2H_2O\}_n$ (4): An aqueous solution (3 mL) of $Cu(NO_3)_2\cdot 3H_2O$ (0.0485 g, 0.2 mmol) was added dropwise to an aqueous solution (13 mL) containing malonic acid (0.1059 g, 1 mmol) and adenine (0.0273 g, 0.2 mmol) with continuous stirring at 80 °C. The resulting solution (pH 2.0) was neutralised with NaOH to obtain a pH of 4.2. Light blue X-ray quality single-crystals were obtained by slow evaporation after two weeks. Yield 51.8 mg (0.09 mmol, 45%). $C_{16}H_{20}CuN_{10}O_{10}$ (575.97): calcd. C 33.37, H 3.50, Cu 11.03, N 24.32; found C 33.20, H 3.61, Cu 10.99, N 24.36. Selected IR data (KBr pellet): $\tilde{\nu}$ = 3416 s [ν(O–H)]; 3222 s [$\nu(NH_2) + 2\delta(NH_2)$]; 3026 s [$\nu(C^8–H + C^2–H)$]; 1702 s [$\nu_{as}$(O–C–O)]; 1652 w [$\nu$(C=C) + $\delta(NH_2)$]; 1556 vs [$\nu(C^4–C^5) + \nu(N^3–C^4–C^5)$]; 1448 m [$\delta(C^2–H + C^8–N^9) + \nu(C^8–H)$]; 1412 m [$\delta(N^1–C^6–H^6)$]; 1364 m [$\nu(C^5–N^7–C^8$]; 1275 m [$\nu(N^9–C^8 + N^3–C^2) + \delta$(C–H) + ν_s(O–C–O)]; 1234 m, 1191 m, 1117 w [$\delta(C^8–H) + \nu(N^7–C^8)$]; 993 m [$\tau(NH_2$]; 941 m, 886 m [$\nu(N^1–C^6) + \tau(NH_2)$]; 799 m, 742 m [$\delta$(O–C–O]; 709 m, 644 w, 617 w (ring deformation); 560 m, 539 m, 520 m, 458 w [ν(M–O + M–N)].

Synthesis of $(H_2ade)_2[Cu(mmal)_2(H_2O)]$ (5): An aqueous solution (5 mL) of $Cu(NO_3)_2\cdot 3H_2O$ (0.0483 g, 0.2 mmol) was added dropwise to an aqueous solution (20 mL) containing methylmalonic acid (0.0484 g, 0.4 mmol) and adenine (0.0271 g, 0.2 mmol) with continuous stirring at 80 °C. The resulting solution (pH 2.5) was neutralised with NaOH to obtain a pH of 5.4. Light blue X-ray quality single-crystals were obtained by slow evaporation after three weeks. Yield 41.0 mg (0.07 mmol, 35%). $C_{18}H_{22}CuN_{10}O_9$ (585.98): calcd. C 36.89, H 3.78, Cu 10.84, N 23.90; found C 36.95,

Table 4. Single-crystal data and structure refinement details for compounds **1**–**5**.

	1	**2**	**3**	**4**	**5**
Formula	$C_8H_{11}N_5NiO_6$	$C_8H_{11}CoN_5O_6$	$C_8H_9CoN_5O_5$	$C_{16}H_{20}CuN_{10}O_{10}$	$C_{18}H_{22}CuN_{10}O_9$
Weight [g mol^{-1}]	331.91	332.15	314.13	575.97	586.01
Crystal system	monoclinic	monoclinic	monoclinic	triclinic	orthorhombic
Space group	$P2_1/c$	$P2_1/c$	$P2_1/c$	$P\bar{1}$	*Pnma*
a [Å]	7.1286(2)	7.144(1)	9.2324(12)	5.0810(2)	9.0641(3)
b [Å]	10.4120(4)	10.587(2)	7.3330(9)	9.4290(7)	19.2927(5)
c [Å]	15.9463(5)	16.108(2)	17.669(2)	11.3840(7)	12.9887(3)
α [°]	90(–)	90(–)	90(–)	91.738(5)	90(–)
β [°]	89.980(3)	89.86(1)	115.204(10)	96.965(4)	90(–)
γ [°]	90(–)	90(–)	90(–)	96.172(4)	90(–)
V [Å^3]	1183.58(7)	1218.3(3)	1082.3(2)	537.71(6)	2271.35(11)
Z	4	4	4	1	4
$\rho_{calcd.}$ [g cm^{-3}]	1.863	1.811	1.928	1.779	1.714
ρ_{obsd} [g cm^{-3}]	1.85(1)	1.80(2)	1.91(2)	1.80(2)	1.70(1)
μ [mm^{-1}]	1.677	1.445	1.614	1.097	1.037
Reflections collected	6533	4819	5019	4264	15545
Unique data/parameters	3451/176	3282/176	2324/172	1692/169	3409/181
R_{int}	0.0381	0.1029	0.0815	0.0287	0.0447
Reflections with $I \geq 2\sigma(I)$	2115	1143	907	1126	2129
Goodness of fit (S)[a]	0.941	0.946	0.955	1.030	0.874
R_1[b]/wR_2 [c] [$I \geq 2\sigma(I)$]	0.0460/0.1099	0.0475/0.0602	0.0459/0.0832	0.0313/0.0743	0.0383/0.0825
R_1/wR_2 [all data]	0.0712/0.1145	0.0943/0.0814	0.1454/0.0951	0.0384/0.0759	0.0729/0.0895

[a] $S = [\sum w(F_o^2 - F_c^2)^2/(N_{obs} - N_{param})]^{1/2}$. [b] $R_1 = \sum||F_o| - |F_c||/\sum|F_o|$. [c] $wR_2 = [\sum w(F_o^2 - F_c^2)^2/\sum wF_o^2]^{1/2}$; $w = 1/[\sigma^2(F_o^2) + (aP)^2]$ where $P = [\max(F_o^2,0) + 2F_c^2]/3$ with $a = 0.0649$ (for **1**), 0.0150 (for **2**), 0.0375 (for **3**), 0.0488 (for **4**) and 0.0514 (for **5**).

H 3.71, Cu 10.89, N 23.88. Selected IR data (KBr pellet): 3422 s [ν(O–H); 3247 s [ν(NH_2) + 2δ(NH_2)]; 3054 s [ν(C^8–H + C^2–H]; 1685 s [ν_{as}(O–C–O]; 1647 w, 1610 s [ν(C=C) + δ(NH_2)]; 1588 s [ν(C^4–C^5) + ν(N^3–C^4–C^5)]; 1450 m [δ(C^2–H + C^8–N^9) + ν(C^8–H)]; 1400 m [δ(N^1–C^6–H^6]; 1274 m [ν(N^9–C^8 + N^3–C^2) + δ(C–H) + ν_s(O–C–O)]; 1240 w, 1180 w, 1109 w [δ(C^8–H) + ν(N^7–C^8)]; 936 m, 914 m, 887 m [ν(N^1–C^6) + τ(NH_2)]; 835 m [δ(O–C–O]; 715 m, 639 m, 618 m (ring deformation); 583 w, 561 w, 539 w, 473 w [ν(M–O + M–N)].

X-ray Structural Studies: Diffraction data were collected at 293(2) K on Oxford Diffraction Xcalibur (**1**, **3**, **4**, **5**) and STOE IPDS (**2**) diffractometers with graphite-monochromated Mo-K_α radiation (λ = 0.71073 Å). Data reduction was performed with the CrysAlis RED[33] and X-RED[34] programs, respectively. Structures were solved by direct methods using the SIR92 program[35] and refined by full-matrix least-squares on F^2 including all reflections (SHELXL97).[36] All calculations were performed using the WINGX crystallographic software package.[37] Crystal parameters and details of the final refinements of compounds **1**–**5** are summarised in Table 4.

CCDC-719156 (for **1**), -719157 (for **2**), -719158 (for **3**), -719159 (for **4**) and -719160 (for **5**) contain the supplementary crystallographic data for this paper. These data can be obtained free of charge from The Cambridge Crystallographic Data Centre via www.ccdc.cam.ac.uk/data_request/cif.

Computational Details: All quantum-mechanical calculations of optimised geometries were carried out in the gas phase using density functional theory with Becke's three-parameter exchange functional[38] along with the Lee–Yang–Parr nonlocal correlation functional (B3LYP).[39] The standard 6-31G(d) basis set was used as implemented in the Gaussian 03 program.[40] It is well known that although the B3LYP functional method might not be suitable for the consistent study of the whole range of the DNA base interactions due to its insufficiency in describing the dispersion interactions, it predicts reliable interaction energies for hydrogen-bonded systems.[41] DFT methods have been shown to give good estimates of the magnetic interactions.[42] A detailed description of the computational strategy adopted in this work to compute the magnetic coupling constant (J_{calc}) values has been described elsewhere.[43] Density functional theory was used to carry out two separate calculations to evaluate the coupling constant of each compound. One calculation was performed to determine the high-spin state and another to determine the low-spin broken symmetry state. The correctness of the latter state was ensured by means of its spin density distribution. The hybrid B3LYP method[38] was used in all calculations as implemented in Gaussian 03,[40] so that the exact Hartree–Fock-type exchange was mixed with Becke's expression for the exchange functional[44] and the Lee–Yang–Parr correlation functional[39] was used. The Gaussian implemented 6-31G(d) basis set was employed throughout this work.

Acknowledgments

This work was supported by the Ministerio de Ciencia e Innovación (MAT2008-05690/MAT) and the Gobierno Vasco (IT-280-07). Sonia Pérez-Yáñez and Javier Cepeda thank the Universidad del País Vasco/Euskal Herriko Unibertsitatea for a predoctoral fellowship (PIFA01/2007/021). The SGI/IZO-SGIker UPV/EHU, financed by the National Program for the Promotion of Human Resources within the National Plan of Scientific Research, Development and Innovation – "Ministerio de Ciencia e Innovación", "Fondo Social Europeo (FSE)" and "Gobierno Vasco/Eusko Jaurlaritza, Dirección de Política Científica" is gratefully acknowledged for generous allocation of computational, X-ray diffraction and magnetic resources.

[1] V. J. Derose, S. Burns, N.-K. Kim, M. Vogt, in: *Comprehensive Coordination Chemistry II* (Eds: J. A. McCleverty, T. J. Meyer),

Elsevier, University of Bern, Switzerland, **2003**, vol. 8, pp. 787–813.
[2] a) A. D. Richards, A. Rodger, *Chem. Soc. Rev.* **2007**, *36*, 471–483; b) H. T. Chifotides, K. R. Dunbar, *Acc. Chem. Res.* **2005**, *38*, 146–156; c) J. A. R. Navarro, B. Lippert, *Coord. Chem. Rev.* **2001**, *222*, 219–250.
[3] M. J. Hannon, *Chem. Soc. Rev.* **2007**, *36*, 280–295.
[4] M. Legraverend, D. S. Grierson, *Bioorg. Med. Chem.* **2006**, *14*, 3987–4006.
[5] a) P. X. Rojas-González, A. Castiñeiras, J. M. González-Pérez, D. Choquesillo-Lazarte, J. Niclós-Gutiérrez, *Inorg. Chem.* **2002**, *41*, 6190–6192; b) F. Zamora, M. Kunsman, M. Sabat, B. Lippert, *Inorg. Chem.* **1997**, *36*, 1583–1587.
[6] a) J. P. García-Terán, O. Castillo, A. Luque, U. García-Couceiro, G. Beobide, P. Román, *Cryst. Growth Des.* **2007**, *7*, 2594–2600; b) J. P. García-Terán, O. Castillo, A. Luque, U. García-Couceiro, G. Beobide, P. Román, *Inorg. Chem.* **2007**, *46*, 3593–3602; c) J. P. García-Terán, O. Castillo, A. Luque, U. García-Couceiro, G. Beobide, P. Román, *Dalton Trans.* **2006**, *7*, 902–911.
[7] C. Ruiz-Pérez, Y. Rodríguez-Martín, M. Hernández-Molina, F. S. Delgado, J. Pasán, J. Sanchiz, F. Lloret, M. Julve, *Polyhedron* **2003**, *22*, 2111–2123.
[8] E. Sletten, *Acta Crystallogr., Sect. B* **1969**, *25*, 1480–1491.
[9] a) P. J. Sanz Miguel, B. Lippert, *Dalton Trans.* **2005**, 1679–1686; b) A. M. Beatty, *Coord. Chem. Rev.* **2003**, *246*, 131–143.
[10] a) J. V. Burda, J. Gu, *J. Inorg. Biochem.* **2008**, *102*, 53–62; b) H. T. Chifotides, K. R. Dunbar, *Acc. Chem. Res.* **2005**, *38*, 146–156.
[11] a) G. Kickelbick, in *Hybrid Materials: Synthesis Characterisation, and Applications*, Wiley-VCH: Weinheim, **2007**; b) P. Horcajada, C. Serre, M. Vallet-Regi, M. Sebban, F. Taulelle, G. Férey, *Angew. Chem. Int. Ed.* **2006**, *45*, 5974–5978; c) J. T. Hupp, K. R. Poeppelmeier, *Science* **2005**, *309*, 2008–2009.
[12] a) M. Fondo, N. Ocampo, A. M. García-Deibe, M. Corbella, M. S. El Fallah, J. Cano, J. Sanmartin, M. R. Bermejo, *Dalton Trans.* **2006**, 4905–4913; b) A. Pajunen, E. Nasakkala, *Finn. Chem. Lett.* **1977**, *4*, 100–103; c) M. Fondo, A. M. García-Deibe, N. Ocampo, J. Sanmartin, M. R. Bermejo, A. L. Llamas-Saiz, *Dalton Trans.* **2006**, 4260–4270.
[13] a) A. Terzis, A. L. Beauchamp, R. Rivest, *Inorg. Chem.* **1973**, *12*, 1166–1170; b) P. de Meester, A. C. Skapski, *J. Chem. Soc. A* **1971**, *13*, 2167–2169; c) J. M. González-Pérez, C. Alarcón-Payer, A. Castiñeiras, T. Pivetta, L. Lezama, D. Choquesillo-Lazarte, G. Crisponi, J. Niclós-Gutiérrez, *Inorg. Chem.* **2006**, *45*, 877; d) J. P. García-Terán, O. Castillo, A. Luque, U. García-Couceiro, P. Román, L. Lezama, *Inorg. Chem.* **2004**, *43*, 4549.
[14] A. Klanicová, Z. Travnicek, I. Popa, M. Cajan, K. Dolezal, *Polyhedron* **2006**, *25*, 1421–1432.
[15] A. Travnicek, Z. Smekal, J. Marel, *Z. Kristallogr.* **1997**, *212*, 123–124.
[16] E. Cubero, N. G. A. Abrescia, J. A. Subirana, F. G. Luque, M. Orozco, *J. Am. Chem. Soc.* **2003**, *125*, 14603–14612.
[17] A. C. Cheng, A. D. Frankel, *J. Am. Chem. Soc.* **2004**, *126*, 434–435.
[18] K. Gotoh, R. Ishikawa, H. Ishida, *Acta Crystallogr., Sect. E* **2007**, *63*, o4433–o4433.
[19] G. Hu, P. D. Gershon, A. E. Hodel, F. A. Quiocho, *Proc. Natl. Acad. Sci.* **1999**, *96*, 7149–7154.
[20] J. Mann, A. Baron, Y. Opoku-Boahen, E. Johansson, G. Parkinson, L. R. Kelland, S. Neidle, *J. Med. Chem.* **2001**, *44*, 138–144.
[21] a) M. E. Curry, D. S. Eggleston, D. J. Hodgson, *J. Am. Chem. Soc.* **1985**, *107*, 8234–8238; b) J. M. Tercero, A. Matilla, M. A. Sanjuan, C. F. Moreno, J. D. Martin, J. A. Walmsley, *Inorg. Chim. Acta* **2003**, *342*, 77–87; c) J. Pasán, J. Sanchiz, F. Lloret, M. Julve, C. Ruiz-Pérez, *CrystEngComm* **2007**, *9*, 478–487.
[22] J. P. García-Terán, O. Castillo, A. Luque, U. García-Couceiro, G. Beobide, P. Román, *Inorg. Chem.* **2007**, *46*, 3593–3602.
[23] A. P. Ginsberg, R. L. Martin, R. W. Brookes, R. C. Sherwood, *Inorg. Chem.* **1972**, *11*, 2884–2889.
[24] D. Sonnenfroh, R. W. Kreilick, *Inorg. Chem.* **1980**, *19*, 1259–1262.
[25] a) F. S. Delgado, M. Hernández-Molina, J. Sanchiz, C. Ruiz-Pérez, Y. Rodríguez-Martín, T. López, F. Lloret, M. Julve, *CrystEngComm* **2004**, *6*, 106–111; b) L. Cañadillas-Delgado, O. Fabelo, J. Pasán, F. S. Delgado, F. Lloret, M. Julve, C. Ruiz-Pérez, *Inorg. Chem.* **2007**, *46*, 7458–7465.
[26] Y. Nishida, S. Kida, *J. Chem. Soc., Dalton Trans.* **1986**, 2633–2640.
[27] V. McKee, M. Zvagulis, C. A. Reed, *Inorg. Chem.* **1985**, *24*, 2914–2919.
[28] M. E. Lines, *J. Chem. Phys.* **1971**, *55*, 2977–2984.
[29] G. A. Baker, G. S. Rushbrooke, H. E. Gilbert, *Phys. Rev.* **1964**, *135*, A1272–A1277.
[30] O. Kahn, in: *Molecular Magnetism*, VCH Publishers, New York, **1993**.
[31] a) F. S. Delgado, J. Sanchiz, C. Ruiz-Pérez, F. Lloret, M. Julve, *Inorg. Chem.* **2003**, *42*, 5938–5948; b) J. Sanchiz, Y. Rodríguez-Martín, C. Ruiz-Pérez, A. Mederos, F. Lloret, M. Julve, *New J. Chem.* **2002**, *26*, 1624–1628; c) C. Ruiz-Pérez, J. Sanchiz, M. Hernández-Molina, F. Lloret, M. Julve, *Inorg. Chem.* **2000**, *39*, 1363–1370; d) D. Chattopadhyay, S. K. Chattopadhyay, P. R. Lowe, *J. Chem. Soc., Dalton Trans.* **1993**, 913–916.
[32] A. Earnshaw, in: *Introduction to Magnetochemistry*, Academic Press, London, **1968**.
[33] *CrysAlis RED*, version 1.170; Oxford Diffraction: Wroclaw, Poland, **2003**.
[34] Stoe & Cie, *STADI4* and *X-RED*, Stoe & Cie GmbH, Darmstadt, Germany, **2002**.
[35] A. Altomare, M. Cascarano, C. Giacovazzo, A. Guagliardi, *J. Appl. Crystallogr.* **1993**, *26*, 343–350.
[36] G. M. Sheldrick, *SHELXL97*, University of Göttingen, Germany, **1997**.
[37] L. J. Farrugia, *WINGX*, A Windows Program for Crystal Structure Analysis, University of Glasgow, UK, **1998**.
[38] A. D. Becke, *J. Chem. Phys.* **1993**, *98*, 5648–5652.
[39] a) C. Lee, W. Yang, R. G. Parr, *Phys. Rev. B* **1988**, *37*, 785–789; b) B. Miehlich, A. Savin, H. Stoll, H. Preuss, *Phys. Lett.* **1989**, *157*, 200–206.
[40] M. J. Frisch, G. W. Trucks, H. B. Schlegel, G. E. Scuseria, M. A. Robb, J. R. Cheeseman, J. A. Montgomery Jr., T. Vreven, K. N. Kudin, J. C. Burant, J. M. Millam, S. S. Iyengar, J. Tomasi, V. Barone, B. Mennucci, M. Cossi, G. Scalmani, N. Rega, G. A. Petersson, H. Nakatsuji, M. Hada, M. Ehara, K. Toyota, R. Fukuda, J. Hasegawa, M. Ishida, T. Nakajima, Y. Honda, O. Kitao, H. Nakai, M. Klene, X. Li, J. E. Knox, H. P. Hratchian, J. B. Cross, V. Bakken, C. Adamo, J. Jaramillo, R. Gomperts, R. E. Stratmann, O. Yazyev, A. J. Austin, R. Cammi, C. Pomelli, J. W. Ochterski, P. Y. Ayala, K. Morokuma, G. A. Voth, P. Salvador, J. J. Dannenberg, V. G. Zakrzewski, S. Dapprich, A. D. Daniels, M. C. Strain, O. Farkas, D. K. Malick, A. D. Rabuck, K. Raghavachari, J. B. Foresman, J. V. Ortiz, Q. Cui, A. G. Baboul, S. Clifford, J. Cioslowski, B. B. Stefanov, G. Liu, A. Liashenko, P. Piskorz, I. Komaromi, R. L. Martin, D. J. Fox, T. Keith, M. A. Al-Laham, C. Y. Peng, A. Nanayakkara, M. Challacombe, P. M. W. Gill, B. Johnson, W. Chen, M. W. Wong, C. Gonzalez, J. A. Pople, *Gaussian 03*, revision C.02, Gaussian, Inc., Wallingford, CT, **2004**.
[41] a) A. K. Rappe, E. R. Bernstein, *J. Phys. Chem. A* **2000**, *104*, 6117–6128; b) O. S. Sukhanov, O. V. Shiskin, L. Gorb, Y. Podolyan, J. Leszczynskii, *J. Phys. Chem. B* **2003**, *107*, 2846–2852; c) A. V. Morozov, T. Kortemme, K. Tsemekhman, D. Baker, *Proc. Natl. Acad. Sci. USA* **2004**, *101*, 6946–6951.
[42] a) J. Cano, P. Alemany, S. Álvarez, M. Verdaguer, E. Ruiz, *Chem. Eur. J.* **1998**, *4*, 476–484; b) M. D. Santana, G. García, M. Julve, F. Lloret, J. Pérez, M. Liu, F. Sanz, J. Cano, G. López, *Inorg. Chem.* **2004**, *43*, 2132–2140; c) E. Ruiz, A.

Rodríguez-Fortea, S. Álvarez, *Inorg. Chem.* **2003**, *42*, 4881–4884.
[43] a) E. Ruiz, J. Cano, S. Álvarez, P. Alemany, *J. Comput. Chem.* **1999**, *20*, 1391–1400; b) E. Ruiz, P. Alemany, S. Álvarez, J. Cano, *J. Am. Chem. Soc.* **1997**, *119*, 1297–1303; c) E. Ruiz, A. Rodríguez-Fortea, J. Cano, S. Álvarez, P. Alemany, *J. Comput. Chem.* **2003**, *24*, 982–989; d) E. Rudberg, P. Salek, Z. Rinkevicius, H. Agren, *J. Chem. Theory Comput.* **2006**, *2*, 981–989.
[44] A. D. Becke, *Phys. Rev. A* **1988**, *38*, 3098–3100.
Received: February 5, 2009
Published Online: April 29, 2009

